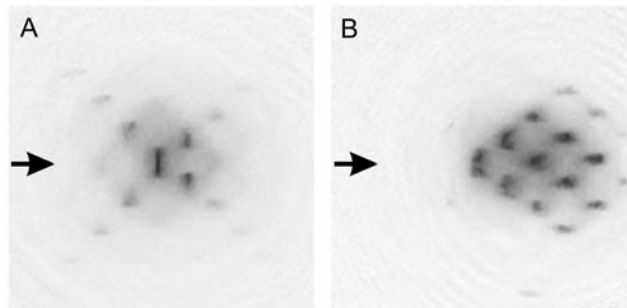


Progress in year 2003

1. The onset of matter-wave amplification in a superradiant Bose-Einstein condensate

We have studied the interaction of short and strong laser pulses with an atomic Bose-Einstein condensate [1]. Light at low intensity is scattered into all directions – this is the well-known case of Rayleigh scattering. Stronger laser pulses can give rise to collective “superradiant” light scattering. In the case of elongated Bose-Einstein condensates, the light is predominantly emitted along the long axis of the condensate in the so-called endfire modes [2]. The recoiling atoms appear as distinct peaks in momentum space corresponding to the momentum transfer of an absorbed pump photon and a superradiantly scattered photon.

Short and intense laser pulses were found to generate patterns of recoiling atoms that were strikingly different from those seen in previous experiments [1]. Superradiantly emitted photons were reabsorbed and re-emitted into the pump beam, leading to atoms, which were recoiling out of the condensate with a velocity component antiparallel to the pump beam. Since this process is non-resonant, it occurs only for short pulse durations. These experiments show that the previous description of superradiance as atomic stimulation was incomplete and that optical stimulation plays a crucial role. The reabsorption of superradiant photons implies that matter wave amplification in superradiant Bose-Einstein condensates is suppressed at early times. Our experiments elucidate the nature of bosonic stimulation in the four-wave mixing of light and atoms and the interplay of optical and atomic stimulation.



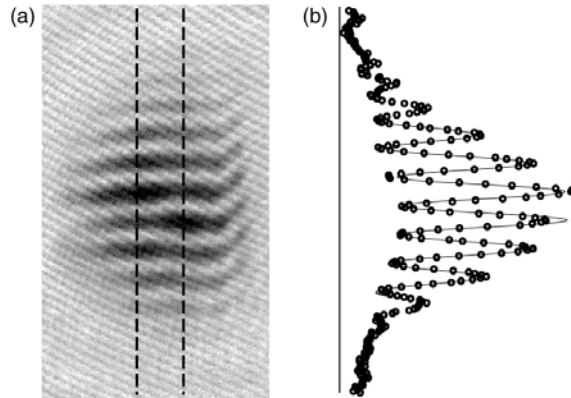
Superradiant scattering of a laser beam (arrow) from a Bose-Einstein condensate in the short-pulse (A) and long-pulse (B) limit. Absorption images of the atomic density distribution were taken after 30 ms of ballistic expansion. In case A, the detuning was 420 MHz and the pulse duration was 6 μ s. In case B, the detuning was -4400 MHz and the pulse duration was 800 μ s. The field of view of both images is 2.0 mm by 2.0 mm, and that of the inset is 120 μ m by 270 μ m.

2. Atom interferometry with Bose-Einstein condensates in a double-well potential

The applicability, accuracy, and sensitivity of atom interferometers may be improved by exploiting the laser-like coherence properties of gaseous Bose-Einstein condensates in combination with the fine manipulation capabilities of atomic microtraps and

waveguides. Current proposals for microtrap and waveguide interferometers utilize double-well potentials for beam splitters and recombiners. To implement a prototype of such schemes, we created a trapped-atom interferometer using gaseous Bose-Einstein condensates coherently split by deforming an optical single-well potential into a double-well potential [3].

Sodium condensates were split by deforming an initially single-well potential into two wells separated by $13\ \mu\text{m}$. To avoid deleterious mean field effects common to traditional in-trap recombination schemes, the relative phase between the two condensates was determined from the spatial phase of the matter wave interference pattern formed upon releasing the atoms from the separated potential wells. The coherence time of the separated condensates was measured to be $5\ \text{ms}$, and was set by technical limitations of our current setup. The large separation between the split potential wells allowed the phase of each condensate to evolve independently and either condensate to be addressed individually.



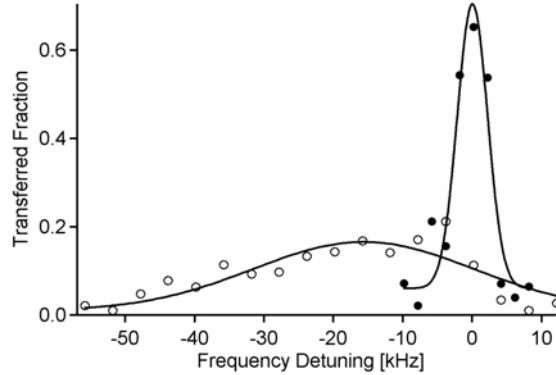
Matter wave interference. (a) Absorption image of condensates released from the optical double-well potential and allowed to expand for $30\ \text{ms}$. The field of view is $600\ \mu\text{m} \times 350\ \mu\text{m}$. (b) Radial density profiles were obtained by integrating the absorption signal between the dashed lines, and typical interference patterns had $> 60\%$ contrast. The spatial phase of the matter wave interference pattern was extracted from the fit shown.

3. Radio-Frequency Spectroscopy of Ultracold Fermions

Radio-frequency techniques were used to study ultracold fermions [4]. By starting with a sample in one quantum state (state 2) and driving it to another state (state 3) we verified the prediction of the absence of mean-field “clock” shifts, the dominant source of systematic error in current atomic clocks based on bosonic atoms. This absence is a direct consequence of fermionic antisymmetry which prevents two atoms in the same state to interact with contact interactions.

Resonance shifts proportional to interaction strengths were observed in a three-level system when the transition between states 2 and 3 was driven in the presence of atoms in a third state (state 1). When the interactions were weak, the observed shifts agreed with theoretical calculations. However, in the strongly interacting regime, these shifts became very small, reflecting the quantum unitarity limit and many-body effects. This insight

into an interacting Fermi gas is relevant for the quest to observe superfluidity in this system.



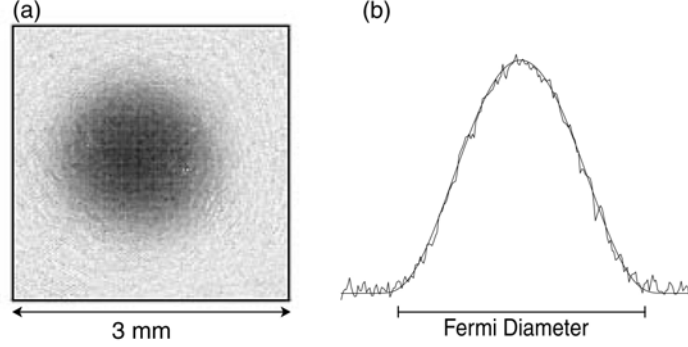
Measurement of the mean-field energy in an interacting Fermi gas. The fraction of atoms transferred by the radio-frequency pulse from state 2 to state 3, with atoms in state 1 absent (solid circles) and present (open circles). The mean-field shift due to the presence of atoms in state 1 is computed from Gaussian fits to the data (solid lines).

4. Fifty-fold improvement in the number of quantum degenerate fermionic atoms

For a long time, the cooling of Fermi gases was lagging behind the studies of atomic Bose-Einstein condensates (BECs) due to the complexity of cooling methods. The Pauli exclusion principle prohibits elastic collisions between identical fermions at ultra-low temperatures, and makes evaporative cooling of spin-polarized fermionic samples impossible. For this reason, cooling of fermions must rely on some form of mutual or sympathetic cooling between two types of distinguishable particles. A key element in fermion cooling is the design of better “refrigerators” for sympathetic cooling.

We have realized evaporative cooling of sodium in the upper hyperfine state ($F=2$) and achieved Bose-Einstein condensates in this state by direct evaporation. Sympathetic cooling of lithium with that cloud decreased losses due to inelastic collisions encountered in earlier experiment with sodium in the lower ($F=1$) state.

This resulted in the production of degenerate Fermi samples comparable in size with the largest alkali BECs [5]. We successfully cooled up to 7×10^7 magnetically trapped ${}^6\text{Li}$ atoms to below half the Fermi temperature (T_F), an improvement in atom number by a factor of 50 over the largest previously reported Fermi sea. Further, in samples containing up to 3×10^7 atoms, we observed temperatures as low as $0.05 T_F$, the lowest ever achieved. At these temperatures, the fractional occupation of the lowest energy state differs from unity by less than 10^{-8} .

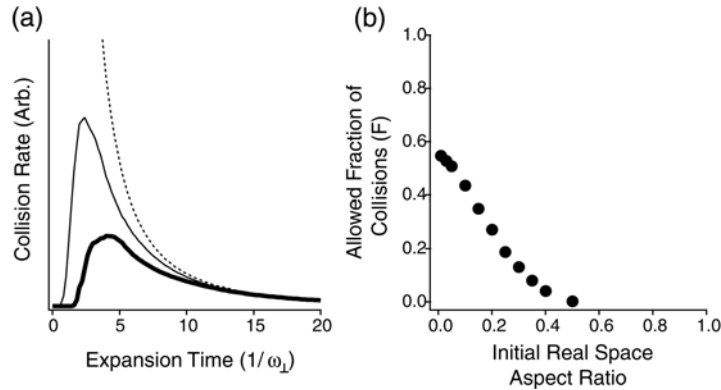


Large and ultra-degenerate Fermi sea. (a) Absorption image of 3×10^7 ${}^6\text{Li}$ atoms released from the trap and imaged after 12 ms of free expansion. (b) Axial (vertical) line density profile of the cloud in (a). A semiclassical fit (thin line) yields a temperature $T = 93 \text{ nK} = 0.05 T_F$. At this temperature, the high-energy wings of the cloud do not extend visibly beyond the Fermi energy, indicated in the figure by the momentum-space Fermi diameter.

5. Collisions in zero temperature Fermi gases

The smoking gun of Bose-Einstein condensation has been the anisotropic “superfluid” expansion of elongated condensates released from the trap. Similarly, superfluid Fermi gas would show anisotropic expansion due to superfluid hydrodynamics [6]. A recent observation of anisotropic expansion of an ultracold, interacting, two-spin fermionic mixture [7] has created considerable excitement and raised the question under what conditions is this expansion a signature of fermionic superfluidity and not of collisional hydrodynamics.

We examined the collisional behavior of two-component Fermi gases released at zero temperature from a harmonic trap [8]. Using a phase-space formalism to calculate the collision rate during expansion, we find that Pauli blocking plays only a minor role for momentum changing collisions. As a result, for a large scattering cross-section, Pauli blocking will not prevent the gas from entering the collisionally hydrodynamic regime. In contrast to the bosonic case, hydrodynamic expansion at very low temperatures is therefore not evidence for fermionic superfluidity.

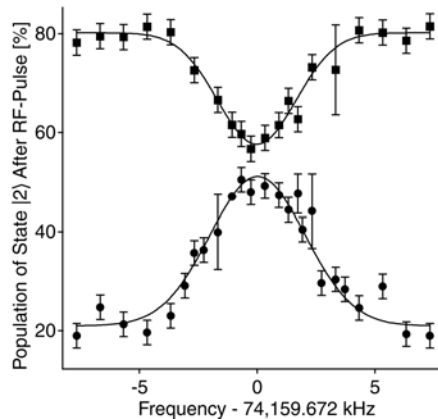


(a) Collision rate as a function of expansion time in the perturbative approximation for an initial aspect ratio of 0.03. Dashed line: total classical collision rate, thin line: classical rate for momentum changing collisions, thick line: collision rate for fermions. (b) Allowed fraction of collisions for a zero-temperature

two-spin Fermi gas. For an initial aspect ratio of 0.05, the fraction is 0.5, and approaches 0.55 for large anisotropy.

6. Spectroscopic insensitivity to cold collisions in a two-state mixture of fermions

We have experimentally addressed the relation between coherence and spectroscopic measurements in a binary mixture of ultracold fermions. We demonstrated that shifts of spectroscopic lines are absent even in a fully decohered binary mixture, in which the particles are distinguishable, and the many-body mean-field energy in the system has developed [9]. We theoretically showed that this is a direct consequence of the coherent nature of the RF excitation, and is not dependent on the coherence of the sample on which spectroscopy is performed. Our calculation intuitively explains both our results for fermions, and previous results for bosons obtained in Boulder [10].

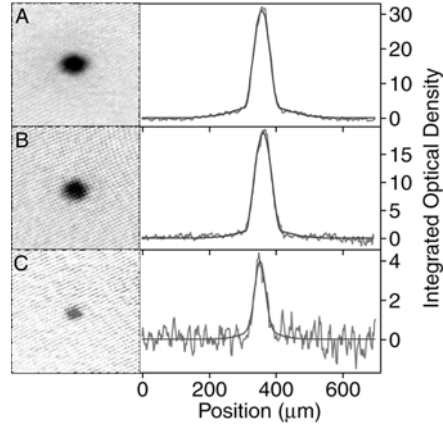


Absence of mean-field shift of an RF transition in a binary Fermi system. The resonance curves were measured for fully decohered 80%/20% two-state mixtures of fermions. The measured frequency difference between the two lines is (34 ± 146) Hz, even though a simple mean-field model would predict a splitting of 20 kHz.

7. Cooling of Bose-Einstein condensates below 500 Picokelvin

The lowest temperatures for trapped atoms are usually achieved in low-density samples. At high densities, interaction effects adversely affect the cooling process and the temperature diagnostics. We have achieved a new record-low temperature of less than 500 picokelvin in a very weak trap using a combination of gravitational and magnetic forces [11]. The partially condensed atomic vapors were adiabatically decompressed by weakening the gravito-magnetic trap to a mean frequency of 1 Hertz, then evaporatively reduced in size to 2500 atoms. This lowered the peak condensate density to 5×10^{10} atoms per cubic centimeter and cooled the entire cloud in all three dimensions to a kinetic temperature of 450 ± 80 picokelvin.

These samples are characterized by a thermal velocity of 1 mm/s, a speed of sound of 100 $\mu\text{m/s}$, and a healing length limited by the 20 μm harmonic oscillator length of the trapping potential. Low temperature and low-density ensembles are important for spectroscopy, metrology, and atom optics. In addition, they are predicted to experience quantum reflection from material surfaces.

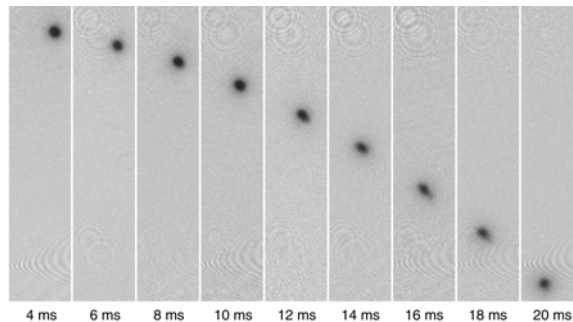


Picokelvin temperature thermometry. Partially condensed atomic vapors confined in the gravito-magnetic trap with (A) 28,000, (B) 16,000, and (C) 2,500 atoms. The one-dimensional cross sections (red) were obtained by integrating the two-dimensional absorption images of the trapped clouds along the y-axis. Bimodal fits (blue) yielded temperatures of (A) 1.05 ± 0.08 nK, (B) 780 ± 50 pK, and (C) 450 ± 80 pK, where the uncertainty is due to the fit of an individual image. The field of view for the absorption images in (A) to (C) is $460 \mu\text{m} \times 460 \mu\text{m}$.

8. Formation of Quantum-Degenerate Sodium Molecules

A current frontier in the field of ultracold gases is the study of ultracold molecules. In 2003, several groups succeeded in converting ultracold atoms into ultracold molecules by magnetically tuning a molecular level close to zero binding energy (Feshbach resonance). Atoms can then form molecules without release of heat.

In our experiment, we produced ultracold sodium molecules from an atomic Bose-Einstein condensate by ramping an applied magnetic field across a Feshbach resonance [12]. More than 10^5 molecules were generated with a conversion efficiency of $\sim 4\%$. High phase-space density could only be achieved by rapidly removing residual atoms, before atom-molecule collisions caused trap loss and heating. This was accomplished by a new technique for preparing pure molecular clouds, where light resonant with an atomic transition selectively “blasted” unpaired atoms from the trap. Time-of-flight analysis of the pure molecular sample yielded an instantaneous phase-space density greater than 20.

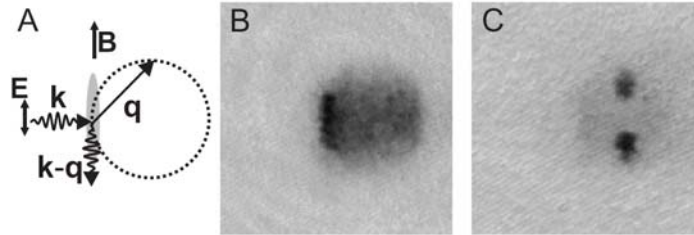


Ballistic expansion of a pure molecular sample. Absorption images of molecular clouds (after reversion to atoms) are shown for increasing expansion time after switching off the optical trap. The small expansion velocity corresponds to a temperature of about 30 nK, characteristic of high phase-space density. The images are taken along the weak axis of the trap. The field of view of each image is $3.0 \text{ mm} \times 0.7 \text{ mm}$.

9. Raman Amplification of Matter Waves

With the realization of coherent, laser-like atoms in the form of Bose-Einstein condensates it has become possible to explore matter-wave amplification, a process in which the number of atoms in a quantum state is amplified due to bosonic stimulation. In previous amplifiers based on superradiant Rayleigh scattering the atoms remained in the same internal state [13, 14], a fact that severely limited the performance since the amplified atoms were scattered out of the final state or served as a gain medium for higher-order processes. We have now realized a Raman atom amplifier in which the gain medium and the amplified atoms are in different internal states [15]. Such a system has analogies to an optical laser in which different transitions are used for pumping and lasing.

The gain mechanism is provided by a polarization grating, a coherence between two different hyperfine states. We observed an exponential growth of this grating and characterized its coherence time.

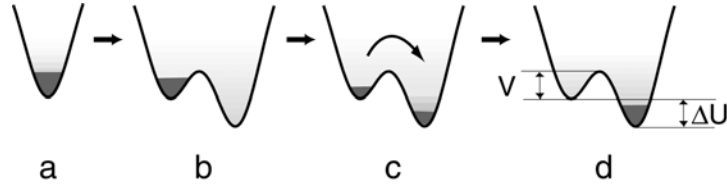


Observation of superradiant Rayleigh scattering. (A) Experimental configuration. A laser beam (wave vector k) is incident perpendicularly to the long axis of the condensate; its electric field vector E is parallel to it and the applied magnetic field B . Each scattering event results in a recoiling atom (momentum $\hbar q$) and a scattered photon (momentum $\hbar(k-q)$). The recoiling atoms lie on a shell of radius $\hbar k$. (B) Spontaneous Rayleigh scattering. The absorption image shows a halo of atoms. The intensity of the beam was 1 mW/cm^2 ; the pulse duration was 1 ms . (C) Superradiant Raman scattering as observed for a beam intensity of 18 mW/cm^2 and a pulse duration of $100 \mu\text{s}$ (the original condensate was fully depleted after $\sim 10 \mu\text{s}$). In both cases the field of view was $1.05 \text{ mm} \times 1.05 \text{ mm}$.

10. Distillation of Bose-Einstein condensates in a double-well potential

The characteristic feature of Bose-Einstein condensation is the accumulation of a macroscopic number of particles in the lowest quantum state. Condensate fragmentation, the macroscopic occupation of two or more quantum states, is usually prevented by interactions [16]. However, multiple condensates may exist in metastable situations. Let's assume that an equilibrium condensate has formed in one quantum state, but now we modify the system allowing for one even lower state. How does the original condensate realize that it is in the wrong state and eventually migrate to the true ground state of the system? What determines the time scale for this equilibration process? This is the situation, which we have experimentally explored by preparing a Bose-Einstein condensate in an optical dipole trap and distilling it into a second empty dipole trap adjacent to the first one [17]. The distillation was driven by thermal atoms spilling over the potential barrier separating the two wells and then forming a new condensate. This process serves as a model system for metastability in condensates, provides a test for

quantum kinetic theories of condensate formation, and also represents a novel technique for creating or replenishing condensates in new locations.



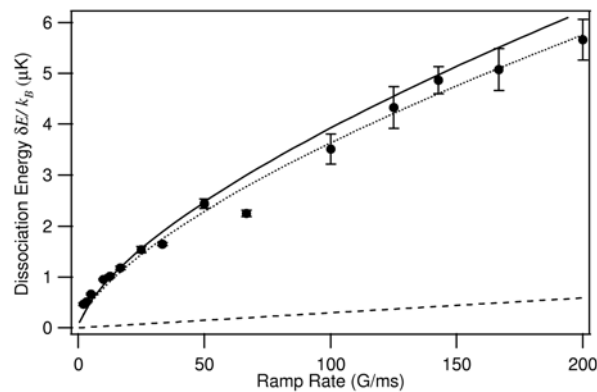
Scheme for distillation of condensates in a double-well potential. (a) Condensates are loaded into the left well. (b) A new ground state is created by linearly ramping the trap depth of the right well from zero to the final value. (c) Atoms transfer into the right well via high-energy thermal atoms, and a new condensate starts to form in the right well. (d) The whole system has equilibrated.

11. Dissociation and Decay of Ultracold Sodium Molecules

We have studied the dissociation and decay of ultracold molecules. Sodium molecules were formed in a highly excited vibrational state by recombining two ultracold atoms [17]. An external magnetic field “tuned” the molecular binding energy close to zero (Feshbach resonance) allowing resonant recombination.

By ramping up the magnetic field, the molecular level was moved into the continuum, and the molecule dissociated. When the magnetic field ramp is very slow, the molecules follow adiabatically and end up in the lowest energy state of the atoms. The dissociation products will populate higher-lying atomic states if the ramp is fast (compared to the strength of the coupling between the molecular and atomic states). Therefore, from the observed dissociation energies, the strength of the atom-molecule coupling could be determined.

The non-linear dependence of the dissociation energy on the ramp speed reflects the Wigner threshold law for the onset of dissociation: The dissociation lifetime decreases when the molecular energy is higher above threshold. Furthermore, inelastic molecule-molecule and molecule-atom collisions were characterized. The rapid inelastic decay imposes a severe limit to further evaporative cooling.

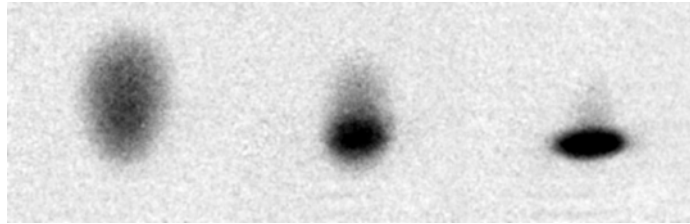


Dissociation energy of sodium molecules as a function of magnetic field ramp rate. The dashed line represents a theoretical prediction of a linear relation, the solid line shows the result of our theory with no free parameters (using a theoretical value for the width ΔB of the Feshbach resonance), and the dotted line shows a curve with ΔB as a fitting parameter.

12. Observation of Bose-Einstein Condensation of Molecules

Molecular condensates could lead to a host of new scientific explorations. These include quantum gases with anisotropic dipolar interactions, tests of fundamental symmetries such as the search for a permanent electric dipole moment, study of rotational and vibrational energy transfer processes, and coherent chemistry, where reactants and products are in coherent quantum superposition states. In November 2003, observation or indirect evidence for Bose-Einstein condensation of molecules was reported by three groups [18-20].

We observed BEC of lithium molecules. When a spin mixture of fermionic ${}^6\text{Li}$ atoms was evaporatively cooled in an optical dipole trap near a Feshbach resonance, the atomic gas was converted into ${}^6\text{Li}$ molecules. Below 600 nK, a Bose-Einstein condensate of up to 900,000 molecules was identified by the sudden onset of a bimodal density distribution. This condensate realizes the limit of tightly bound fermion pairs in the crossover between BCS superfluidity and Bose-Einstein condensation.



Observation of Bose-Einstein condensation in a molecular gas. Shown are three single-shot absorption images after 6 ms of ballistic expansion for progressively lower temperatures (left to right). The appearance of a dark spot marks the onset of BEC. The field of view for each image is $1.4 \times 1.4 \text{ mm}^2$.

1. D. Schneble, Y. Torii, M. Boyd, E.W. Streed, D.E. Pritchard, and W. Ketterle, *The Onset of Matter-Wave Amplification in a Superradiant Bose-Einstein Condensate*, *Science* **300**, 475 (2003).
2. S. Inouye, A.P. Chikkatur, D.M. Stamper-Kurn, J. Stenger, D.E. Pritchard, and W. Ketterle, *Superradiant Rayleigh scattering from a Bose-Einstein condensate*, *Science* **285**, 571 (1999).
3. Y. Shin, M. Saba, T. Pasquini, W. Ketterle, D.E. Pritchard, and A.E. Leanhardt, *Atom interferometry with Bose-Einstein condensates in a double-well potential*, *Phys. Rev. Lett.* **92**, 050405 (2004).
4. S. Gupta, Z. Hadzibabic, M.W. Zwierlein, C.A. Stan, K. Dieckmann, C.H. Schunck, E.G.M.v. Kempen, B.J. Verhaar, and W. Ketterle, *RF Spectroscopy of Ultracold Fermions*, *Science* **300**, 1723 (2003).
5. Z. Hadzibabic, S. Gupta, C.A. Stan, C.H. Schunck, M.W. Zwierlein, K. Dieckmann, and W. Ketterle, *Fifty-fold improvement in the number of quantum degenerate fermionic atoms*, *Phys. Rev. Lett.* **91**, 160401 (2003).
6. C. Menotti, P. Pedri, and S. Stringari, *Expansion of an interacting Fermi gas*, *Phys. Rev. Lett.* **89**, 250402 (2002).
7. K.M. O'Hara, S.L. Hemmer, M.E. Gehm, S.R. Granade, and J.E. Thomas, *Observation of a Strongly Interacting Degenerate Fermi Gas of Atoms*, *Science* **298**, 2179 (2002).
8. S. Gupta, Z. Hadzibabic, J.R. Anglin, and W. Ketterle, *Collisions in zero temperature Fermi gases*, *Phys. Rev. Lett.* **92**, 100401 (2004).
9. M.W. Zwierlein, Z. Hadzibabic, S. Gupta, and W. Ketterle, *Spectroscopic insensitivity to cold collisions in a two-state mixture of fermions*, *Phys. Rev. Lett.* **91**, 250404 (2003).
10. D.M. Harber, H.J. Lewandowski, J.M. McGuirk, and E.A. Cornell, in *Proceedings of the XVIII International Conference on Atomic Physics*, edited by H.R. Sadeghpour, E.J. Heller, and D.E. Pritchard (World Scientific, Cambridge, Massachusetts, 2003) p. 3.
11. A.E. Leanhardt, T.A. Pasquini, M. Saba, A. Schirotzek, Y. Shin, D. Kielpinski, D.E. Pritchard, and W. Ketterle, *Cooling of Bose-Einstein condensates below 500 Picokelvin*, *Science* **301**, 1513 (2003).

12. K. Xu, T. Mukaiyama, J.R. Abo-Shaeer, J.K. Chin, D.E. Miller, and W. Ketterle, *Formation of Quantum-Degenerate Sodium Molecules*, Phys. Rev. Lett. **91**, 210402 (2003).
13. S. Inouye, T. Pfau, S. Gupta, A.P. Chikkatur, A. Görlitz, D.E. Pritchard, and W. Ketterle, *Observation of phase-coherent amplification of atomic matter waves*, Nature **402**, 641 (1999).
14. M. Kozuma, Y. Suzuki, Y. Torii, T. Sugiura, T. Kuga, E.W. Hagley, and L. Deng, *Phase coherent amplification of matter waves*, Science **286**, 2309 (1999).
15. D. Schneble, G.K. Campbell, E.W. Streed, M. Boyd, D.E. Pritchard, and W. Ketterle, *Raman Amplification of Matter Waves*, preprint cond-mat/0311138.
16. P. Nozières, *Some Comments on Bose-Einstein Condensation*, in *Bose-Einstein Condensation*, edited by A. Griffin, D.W. Snoke, and S. Stringari (Cambridge University Press, Cambridge, 1995) p. 15.
17. Y. Shin, M. Saba, A. Schirotzek, T.A. Pasquini, A.E. Leanhardt, D.E. Pritchard, and W. Ketterle, *Distillation of Bose-Einstein condensates in a double-well potential* **92**, 150401 (2004).
18. M. Greiner, C.A. Regal, and D.S. Jin, *Emergence of a molecular Bose-Einstein condensate from a Fermi gas*, Nature **426**, 537 (2003).
19. M.W. Zwierlein, C.A. Stan, C.H. Schunck, S.M.F. Raupach, S. Gupta, Z. Hadzibabic, and W. Ketterle, *Observation of Bose-Einstein Condensation of Molecules*, Phys. Rev. Lett. **91**, 250401 (2003).
20. S. Jochim, M. Bartenstein, A. Altmeyer, G. Hendl, S. Riedl, C. Chin, J. Hecker Denschlag, and R. Grimm, *Bose-Einstein Condensation of Molecules*, Science **302**, 2101 (2003).